Polarizability tensor invariants of H_2, HD, and D_2

Ankit Raj, Hiro-o Hamaguchi, and Henryk A. Witek

Citation: The Journal of Chemical Physics **148**, 104308 (2018); doi: 10.1063/1.5011433
View online: https://doi.org/10.1063/1.5011433
View Table of Contents: http://aip.scitation.org/toc/jcp/148/10
Published by the American Institute of Physics

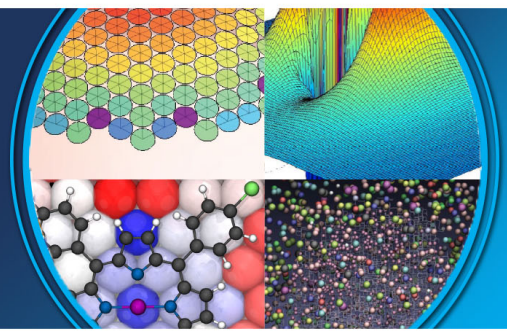

Polarizability tensor invariants of H_2, HD, and D_2

Ankit Raj, Hiro-o Hamaguchi, and Henryk A. Witek[a)]
Department of Applied Chemistry and Institute of Molecular Science, National Chiao Tung University, Hsinchu 30010, Taiwan

(Received 1 November 2017; accepted 21 February 2018; published online 14 March 2018)

We report an exhaustive compilation of wavelength-dependent matrix elements over the mean polarizability ($\bar{\alpha}$) and polarizability anisotropy (γ) operators for the rovibrational states of the H_2, HD, and D_2 molecules together with an accompanying computer program for their evaluation. The matrix elements can be readily evaluated using the provided codes for rovibrational states with $J = 0$–15 and $v = 0$–4 and for any laser wavelengths in the interval 182.25–1320.6 nm corresponding to popular, commercially available lasers. The presented results substantially extend the scope of the data available in the literature, both in respect of the rovibrational transitions analyzed and the range of covered laser frequencies. The presented detailed tabulation of accurate polarizability tensor invariants is essential for successful realization of our main long-term goal: developing a universal standard for determining absolute Raman cross sections and absolute Raman intensities in experimental Rayleigh and Raman scattering studies of molecules. *Published by AIP Publishing.* https://doi.org/10.1063/1.5011433

I. INTRODUCTION

The concept of polarizability plays an important role in the study of light-matter interactions, particularly in the process of scattering of light by atoms and molecules. The theory relating the depolarization ratios in Rayleigh and Raman scattering and the band intensities in the rotational Raman spectrum to the vibrationally and rotationally averaged invariants of the polarizability tensor was developed by Placzek.[1] This theory is valid for molecules with a non-degenerate ground state and for sources of electromagnetic radiation with energy ranges not covering absorption and resonance processes. In particular, it is applicable for the description of scattering of visible light by the hydrogen molecule and its isotopologues. Owing to the simplicity of these systems, H_2, HD, and D_2 are of great interest for Raman spectroscopy since the invariants of the polarizability tensor can be determined both from theory and from the experimentally measured Rayleigh depolarization ratios. Accurate experimental measurements of Raman intensities and Raman depolarization ratios for rovibrational transitions in H_2, HD, and D_2 accompanied by accurate theoretical *ab initio* determination of those quantities can provide a universal standard for determining absolute Raman cross sections[2,3] and absolute Raman intensities[4,5] needed for quantitative Raman spectroscopy,[18,20,87,88,105] calibration of Raman spectrometers,[6,7] determination of rovibrational population distributions,[8–10] and more. Calibrated Raman spectrometers allow for precise experiments, for example, determining experimental Raman cross sections[3,11–13] and temperature determination using anti-Stokes and Stokes Raman intensities.[5,14–23] Our long-term goal is to develop such a universal standard based on the rovibrational Raman transitions in various isotopologues of the hydrogen molecule. The current study, reporting numerical codes capable of computing accurate wavelength-dependent transition matrix elements over the mean polarizability ($\bar{\alpha}$) and polarizability anisotropy (γ)[24] operators for any incident light wavelength in the interval 182.25–1320.6 nm corresponding to popular commercially available lasers usually employed in Raman spectroscopy and for the rovibrational states of the H_2, HD, and D_2 molecules with $J = 0$–15 and $v = 0$–4 (for the $X^1\Sigma_g^+$ electronic state), constitutes the first step in this direction.

Several theoretical techniques were used in the past for computing the polarizability of the hydrogen molecule and its isotopologues. Static polarizability was calculated for H_2 by Kołos and Wolniewicz,[25] using the variation-perturbation method. Ford and Browne[26] used sum-over states method with the configuration interaction wave functions to calculate polarizability for hydrogen at several different wavelengths. Rychlewski[27] performed state-of-the-art calculations using the variation-perturbation method for the wavelength-dependent polarizability components of HD and D_2. Schwartz and Le Roy[28] computed the rovibrational wave functions for six isotopic forms of H_2 using a clamped nuclei potential[29] with relativistic,[30] radiative,[31] and scaled adiabatic corrections.[30,32] Using those rovibrational wave functions and *ab initio* polarizability tensors determined by Rychlewski, they calculated the matrix elements over the mean polarizability ($\bar{\alpha}$) and polarizability anisotropy (γ) operators at the excitation wavelength of 488 nm.

In spite of the continued interest[3–7,10,28,33–37,102,106] in the polarizability of the molecular hydrogen and in the associated matrix elements, the available literature on the subject is limited to the laser excitation wavelengths common decades back. Furthermore, the full set of matrix elements required for a detailed analysis of Raman bands, even for the ground vibrational state, is not available in the literature. This paper is concerned with theoretical determination of isotropic and anisotropic invariants of frequency-dependent polarizability

[a)]hwitek@mail.nctu.edu.tw

for H_2, HD, and D_2 together with their matrix elements relevant for scattering studies of these molecules in their ground electronic state. The polarizability invariants, mean polarizability $\bar{\alpha} = (2\alpha_\perp + \alpha_\parallel)/3$ and polarizability anisotropy $\gamma = \alpha_\parallel - \alpha_\perp$, computed using *ab initio* techniques on a dense grid of interatomic distances, have been used together with the set of rovibrational wave functions to evaluate the corresponding matrix elements for the electronic ground state $X^1\Sigma_g^+$ of H_2, HD, and D_2. The values of the $\bar{\alpha}$ and γ matrix elements can be computed over the set of rovibrational wave functions with $J = 0$–15 and $v = 0$–4, which have been determined by solving numerically the radial-nuclear equation for H_2, HD, and D_2 using the clamped nuclei potential energy surface with adiabatic, relativistic, and radiative corrections obtained by Wolniewicz.[38] The actual values of some of the $\bar{\alpha}$ and γ matrix elements evaluated for a set of 52 common laser wavelengths are tabulated in the supplementary material. The computed matrix elements compare well to the previous theoretical and experimental results available from the literature, allowing in some cases to identify numerical errors in the previously published results. A detailed analysis of various sources of errors in our computational procedure, presented in the supplementary material, allows for establishing approximate error bars for the presented results.

The computational protocol reported here has been implemented in two equivalent FORTRAN and Python programs, which can be used to compute the matrix elements over four operators: polarizability perpendicular to the internuclear axis ($\alpha_\perp$), polarizability parallel to the internuclear axis ($\alpha_\parallel$), mean polarizability ($\bar{\alpha} = (2\alpha_\perp + \alpha_\parallel)/3$), and polarizability anisotropy ($\gamma = \alpha_\parallel - \alpha_\perp$) for H_2, HD, and D_2. These programs are self-contained and use as input the precalculated data, consisting of the distance- and frequency-dependent polarizability tensor components and rovibrational wave functions. These programs together with the set of data files are openly accessible on GitHub[39] and in the supplementary material as a zipped directory.

II. COMPUTATIONAL DETAILS

A. Polarizability calculations

Static and dynamic polarizability tensor components ($\alpha_\parallel$ and $\alpha_\perp$) for H_2 have been calculated on a grid of 176 points spanning from 0.2 a.u. to 12.0 a.u. with a step size (Δr) of 0.05 a.u. from [0.2, 0.35] a.u., Δr = 0.025 a.u. from [0.35, 4.0] a.u., Δr = 0.2 a.u. from [4.0, 6.0] a.u., Δr = 0.25 a.u. from [6.0, 8.0] a.u., and Δr = 0.5 a.u. from [8.0, 12.0] a.u. The calculations have been performed using the CCSD linear response function methodology[40] of Christiansen *et al.* with the DALTON *ab initio* quantum chemistry package.[41] The distance-dependent dynamic polarizabilities have been calculated for 44 wavelengths almost uniformly distributed over the interval 182.25–1320.6 nm; a detailed list of these wavelengths is given in the file freq.txt (in hartree) given as part of the supplementary material.

The molecular basis set used in our calculations has composite character and consists of the hydrogen's atomic aug-mcc-pV6Z basis set[42] of Mielke *et al.* downloaded from the EMSL basis set database[43,44] and an additional bond function basis constructed by us and described in detail below. The original attempt, to compute the polarizabilities using the family of the aug-mcc-pVnZ basis sets[42] and extrapolate the results to the complete basis set limit, was unsuccessful. The extrapolated static polarizabilites showed unacceptably large deviations from the very accurate explicitly correlated results reported previously by Rychlewski.[45] The main reason for this behavior is associated with a very slow convergence of the polarizability (particularly its perpendicular component) with respect to the size of the aug-mcc-pVnZ basis set; for details, see Fig. 1. Even in the largest employed basis, aug-mcc-pV7Z, the difference to the results of Rychlewski is quite substantial and irregular with respect to the H–H interatomic distance. An extension of the aug-mcc-pVnZ basis sets to $n > 7$ is impractical due to the prohibitive computational time associated with such calculations.

The solution to this problem has been found in a form of an additional bond function basis used in combination with the aug-mcc-pV6Z basis set.[42] Atomic orbitals (AOs) forming aug-mcc-pV6Z are centered on the nuclei, failing to reproduce sufficiently accurately molecular orbitals (MOs) at regions away from the nuclei. The inclusion of bond functions, i.e., basis functions centered on certain points along the H–H bond, has been found to improve the situation considerably. The concept of bond functions (also referred to as the mid-bond functions) is not new,[46–50] also in the context of H_2.[51–53] In our calculations, we have observed that the deficiencies of the atomic basis sets can be easily counterbalanced by including a few additional bond functions with low angular momentum and appropriately selected exponents. We have systematically tested the effect of including the bond functions (BFs) on the values of polarizability of H_2 over the full range of the interatomic H–H distances and discovered the following regularities:

- Centering the bond functions on multiple equally spaced points along the H–H bond improves the

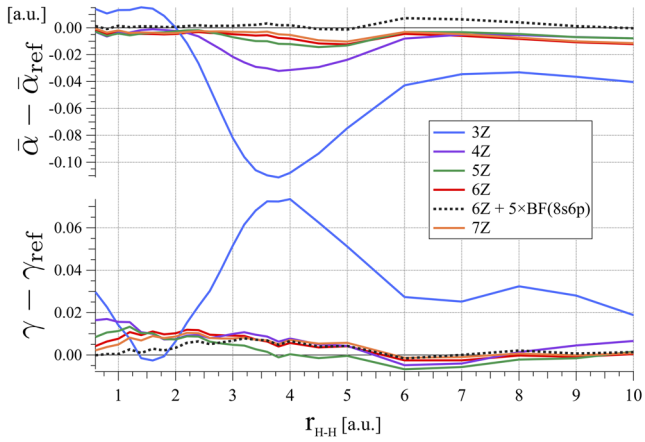

FIG. 1. The values of $\bar{\alpha} - \bar{\alpha}_{ref}$ and $\gamma - \gamma_{ref}$ for the static polarizabilities of H_2 as a function of internuclear distance. The mean polarizability $\bar{\alpha} = (\alpha_\parallel + 2\alpha_\perp)/3$ and polarizability anisotropy $\gamma = \alpha_\perp - \alpha_\parallel$ are computed using the CCSD methodology with the aug-mcc-pVnZ basis sets (shortly nZ) and a composite aug-mcc-pV6Z + 5 × BF (8s6p) basis set [shortly 6Z + 5 × BF (8s6p); for details, see text]. The reference values $\bar{\alpha}_{ref}$ and γ_{ref} are taken from the work of Rychlewski (Ref. 45).

description of polarizability. In our final calculations, we use bond functions centered at five equidistant points between the two nuclei. (For details, see Fig. F2 in the supplementary material and the discussion therein.)

- The most important bond functions required for adequate description of polarizability are those with the angular momentum p. We have found in numerous tests that the saturated BF p-basis is well represented by six even-tempered[54,55] exponents obtained from the formula $\alpha\beta^{1-k}$ with $\alpha = 2.520$, $\beta = 3$, and $k = 1$–6. The BF s-basis, represented in our calculations by eight even-tempered exponents generated by $\alpha = 1.851\,851\,9$ and $\beta = 3$, has much smaller effect. The effect of BF-bases with higher angular momenta is insignificant at shorter internuclear distances and for the purpose of the current study can be neglected. Further discussion is given in Sec. S4 of the supplementary material, particularly in Fig. F4.
- The use of the aug-mcc-pV6Z and aug-mcc-pV7Z bases in the H_2 calculations results in a molecular basis containing 254 and 378 functions, respectively. The number of basis functions for the composite aug-mcc-pV6Z + 5BF bases is 384, but the elimination of linearly dependent components reduces its size to approximately 280 functions at short internuclear separations and 310 functions at long interatomic separations, producing an effective basis only incrementally larger than aug-mcc-pV6Z but of much better accuracy. The performance of various basis sets is visualized in Fig. 2, where we plot the static values of $\alpha_\parallel$, $\alpha_\perp$, γ, and $\bar{\alpha}$ computed with various bases at the equilibrium H–H distance of 1.4 a.u. and compare it against the accurate values reported earlier by Rychlewski.[45]

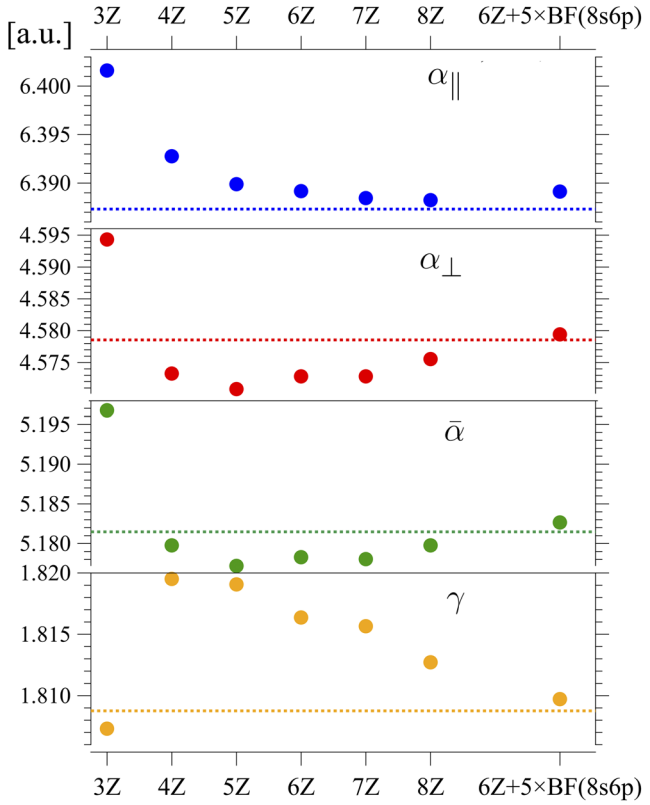

FIG. 2. Static polarizabilities ($\alpha_\parallel$ and $\alpha_\perp$) and its invariants [$\bar{\alpha} = (\alpha_\parallel + 2\alpha_\perp)/3$ and $\gamma = \alpha_\perp - \alpha_\parallel$] for H_2 at $r = 1.4$ a.u. calculated with CCSD using the aug-mcc-pVnZ basis sets (shortly nZ) and a composite aug-mcc-pV6Z + 5 × BF (8s6p) basis set [shortly 6Z + 5 × BF (8s6p); for details, see text]. The results are compared against accurate explicitly correlated results of Rychlewski (Ref. 45) represented as dotted horizontal lines.

B. Rovibrational wave functions

The rovibrational wave functions $\psi_{v,J}$ and energy levels $E_{v,J}$ have been determined numerically by solving the radial nuclear equation

$$\left[\frac{-1}{r^2}\frac{\partial}{\partial r}\frac{r^2}{2\mu}\frac{\partial}{\partial r} + \frac{J(J+1)}{2\mu r^2} + V(r)\right]\psi_{v,J} = E_{v,J}\psi_{v,J} \quad (1)$$

(for details, see Sec. S5 in the supplementary material) on a discrete grid of 2951 equidistant points in the interval 0.2–12.0 a.u. The action of the kinetic energy operator in Eq. (1), involving first and second derivatives, has been evaluated using 5-point difference formulas. The potential energy curve $V(r)$ has been adapted from the work of Wolniewicz.[38] The potential computed by Wolniewicz has four components: the nonrelativistic potential consisting of 670 points, the relativistic correction and adiabatic correction components consisting of 56 points both, and the radiative correction component consisting of 54 points. Each component has been separately evaluated at the finer internuclear distance grid using cubic spline interpolation, and eventually the components have been combined to produce the potential $V(r)$ in Eq. (1). The Hamiltonian matrix has been diagonalized separately for every value of $J = 0$–15 and for different values of reduced masses μ corresponding to H_2, HD, and D_2, yielding the rovibrational levels ($E_{v,J}$) and wave functions ($\psi_{v,J}$). The values of physical constants[56] used to compute the reduced masses are $m_e = 1$ a.u., $m_p = 1836.152\,673\,89\ m_e$, and $m_d = 3670.482\,967\,85\ m_e$. The vibrational levels obtained in this way are accurate to about 1 cm^{-1}, where 1 cm^{-1} = 1/219 474.631 370 2 hartree[56] (for details, see Tables T25–T29 in the supplementary material, where comparisons of dissociation and transition energies with existing literature data[57–68] are given). Note that more accurate methods of determining vibrational wave functions and eigenlevels are available,[57,58] but for the present purpose the accuracy of the rovibrational wave functions obtained here is more than satisfactory. More accurate methods of computing the rovibrational wave functions might be useful in the future when more accurate polarizabilities are available. The calculations have been performed using the Igor Pro[69] software, running custom written procedures. The rovibrational wave functions ($\psi_{v,J}$) determined here have been interpolated over the interval 0.2–12.0 a.u. using a cubic spline representation, to be used in further calculations of appropriate matrix elements in Sec. II C.

C. Determination of the γ and $\bar{\alpha}$ matrix elements

The matrix elements over the operators $\alpha_\parallel$, $\alpha_\perp$, $\bar{\alpha}$, and γ have been computed for the rovibrational wave functions of H_2, HD, and D_2 with $v, v' = 0$–4 and $J, J' = 0$–15 using the

following formula:

$$\langle \psi_{v',J'} | \Omega | \psi_{v,J} \rangle = \int_{r_{\min}}^{r_{\max}} \psi_{v',J'} \Omega \, \psi_{v,J} r^2 dr, \qquad (2)$$

where Ω stands either for $\alpha_{\parallel}$, $\alpha_{\perp}$, $\bar{\alpha}$, or γ having the lower integration limit, $r_{\min}$ = 0.2 a.u. and the upper integration limit, $r_{\max}$ = 4.48 a.u., selected such that both the involved rovibrational wave functions effectively vanish beyond this interval. The integral has been evaluated numerically using the adaptive Gauss-Kronrod-Patterson quadrature,[70,71] as implemented in the dqng.f subroutine of QUADPACK[72] and independently by a 100-point Gauss-Legendre quadrature.[73] The values of the both rovibrational wave functions and the polarizability invariants at the quadrature points have been determined from the cubic spline representations of each quantity. The numerical accuracy of the integration and interpolation schemes used by us is around 10^{-6} and is not an important factor, limiting the accuracy of the computed matrix elements, which are correct to about 10^{-3} due to inaccuracies in the computed values of $\alpha_{\parallel}$ and $\alpha_{\perp}$.

III. RESULTS

The distance- and frequency-dependent polarizability invariants γ and $\bar{\alpha}$ are represented as 2-D surfaces in Fig. 3.

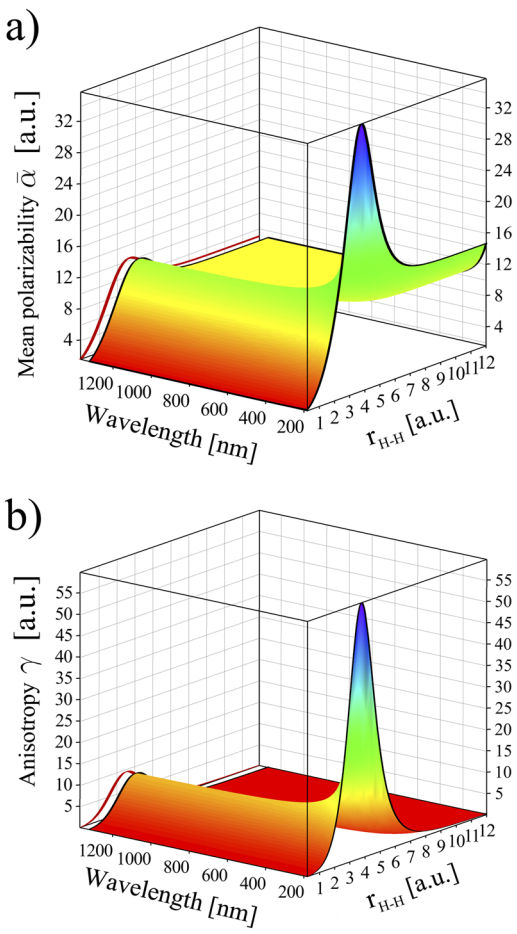

FIG. 3. Wavelength dependent mean polarizability $\bar{\alpha}$ and polarizability anisotropy γ of H_2, HD, and D_2 as a function of the internuclear distance. Frequency independent (static) values are represented using a thick red line.

These plots are identical for all the three molecules owing to their same electronic structure. It is observed that both mean polarizability $\bar{\alpha}$ and polarizability anisotropy γ are smooth functions over both the wavelength and internuclear distance. The sharp feature observed in both plots at the shortest wavelength is a harbinger of the resonance occurring at shorter wavelengths. For longer wavelengths, the dynamic polarizability converges smoothly to the static polarizability, which is depicted using a thick red line in Fig. 3. To facilitate a comparison with previous work, the computed values of static polarizability at various distances over the interval 0.5–12.0 a.u. are listed in Table T17 in the supplementary material.

The matrix elements over the operator $\bar{\alpha}$ computed for the ground electronic state ($X^1\Sigma_g^+$) of H_2, HD, and D_2 are tabulated in Tables T1–T6 under Sec. S1 of the supplementary material. Tables T1, T3, and T5 list the values of the mean polarizability $\bar{\alpha}$, averaged over the ground ($v = 0, J = 0$) and the first vibrationally excited ($v = 1, J = 0$) states relevant in the context of Rayleigh scattering in the columns two and three. The remaining columns list the matrix elements for the $\Delta v = 1$, $\Delta J = 0$ rovibrational transitions pertinent to the Raman intensities of the Q1-branch. Tables T2, T4, and T6 list similar values for the matrix elements connecting the $v = 1$ and $v = 2$ states relevant for the Q2-branch.

The matrix elements over the operator γ computed for H_2, HD, and D_2 are tabulated in Tables T7–T15 under Sec. S2 of the supplementary material. Tables T7, T10, and T13 contain matrix elements for $v = 0$ and Tables T8, T11, and T14 contain matrix elements for $v = 1$, while Tables T9, T12, and T15 have the matrix elements for $v = 2$. These matrix elements are tabulated for the $\Delta v = 0$, $\Delta J = \pm 2$ rovibrational transitions pertinent to the Raman intensities of the O- and S-branches. The maximal value of J in the initial state is set to eight in all the tables. For completeness, Tables T7–T15 give also the value of the $\gamma_{v0,v0}$ matrix element, derivable from experimental data.

The quantities derived here are the key ingredients in modeling and quantitative assessment of the experimental Raman spectra of H_2, HD, and D_2. The remaining ingredients such as Boltzmann distribution factors, nuclear spin degeneracies, and Placzek-Teller coefficients are not discussed here. The matrix elements reported in Tables T1–T15 in the supplementary material are the absolute values given in atomic units. Conversion factors[74] to other units are listed in Table T16 of the supplementary material.

IV. DISCUSSION

The most extensive tabulation of polarizability, its invariants, and the associated matrix elements for H_2, HD, and D_2 available in the literature was given by Rychlewski in a series of papers[27,45,76] published in the early 1980s. Rychlewski[27] presented frequency-dependent diagonal matrix elements for HD and D_2 and off-diagonal matrix elements for H_2, extending an earlier study of Bishop and Cheung,[75] who reported the diagonal matrix elements for H_2. Unfortunately, these results cover only a portion of data needed to explain all the experimental[77] Raman transitions for H_2, HD, and D_2 detectable with modern Raman spectrometers. Publication of our data

fills this gap, substantially extending the scope of previous investigations, both in respect of rovibrational states covered and the reported laser frequencies. The quality of our results is similar to the quality of the existing data.[27,75] In cases, where the discrepancies between our results and the existing data are found not to be negligible, we are able to show that these differences originate from numerical errors in the work of Rychlewski;[27] details are given below. An accuracy assessment of our results is presented in Fig. 4, where we compare all the available matrix elements given by Rychlewski[27] and Bishop and Cheung[75] with analogous results obtained from our calculations by plotting the differences between both sets of data as a function of laser wavelength for the following matrix elements: $\langle 0, J|\Omega|0, J\rangle$ with $J = 0$–4 for H_2 and with $J = 0$–6 for HD and D_2, and $\langle 0, 0|\Omega|1, 0\rangle$ and $\langle 0, J|\Omega|0, J+2\rangle$ with $J = 0$–2 for H_2, where Ω denotes either $\bar{\alpha}$ or γ.

Most of our matrix elements agree with the analogous results given previously by Rychlewski[27] and Bishop and Cheung[75] up to 0.2%. The following exceptions have been identified and analyzed:

- Large discrepancies for the values of $\langle 0, 5|\gamma|0, 5\rangle$ and $\langle 0, 6|\gamma|0, 6\rangle$ for D_2 at 237.93 nm result from an error in the tabulation of matrix elements in Table IV of Ref. 27, where for the wavelength of 2379.3 Å instead of $\langle 0, 5|\gamma|0, 5\rangle$ and $\langle 0, 6|\gamma|0, 6\rangle$ the values of $\langle 0, 6|\gamma|0, 6\rangle$ and $\langle 0, 7|\gamma|0, 7\rangle$ were mistakenly reported.
- Large discrepancies for the matrix elements $\langle 0, J|\gamma|0, J\rangle$ of HD with $J = 0$–6 for the following frequencies 182.26, 404.77, 407.90, 435.96, and 546.23 nm originate from erroneous values of the matrix elements given in Table III of Ref. 27. This can be seen easily from the plot given in Fig. 5, where we show the difference $\langle 0, J|\gamma|0, J\rangle^{\mathrm{HD}} - \langle 0, J|\gamma|0, J\rangle^{\mathrm{D2}}$ for $J = 0$ as a function of laser wavelength for our data (red circles) and Rychlewski's results (blue circles). For all the reported laser wavelengths but five (182.26, 404.77, 407.90, 435.96, and 546.23 nm), both sets of data change smoothly in a similar and predictable way. For the remaining five wavelengths, our data behave smoothly, occupying natural positions on the line demarcated by other wavelengths, while the data of Rychlewski show

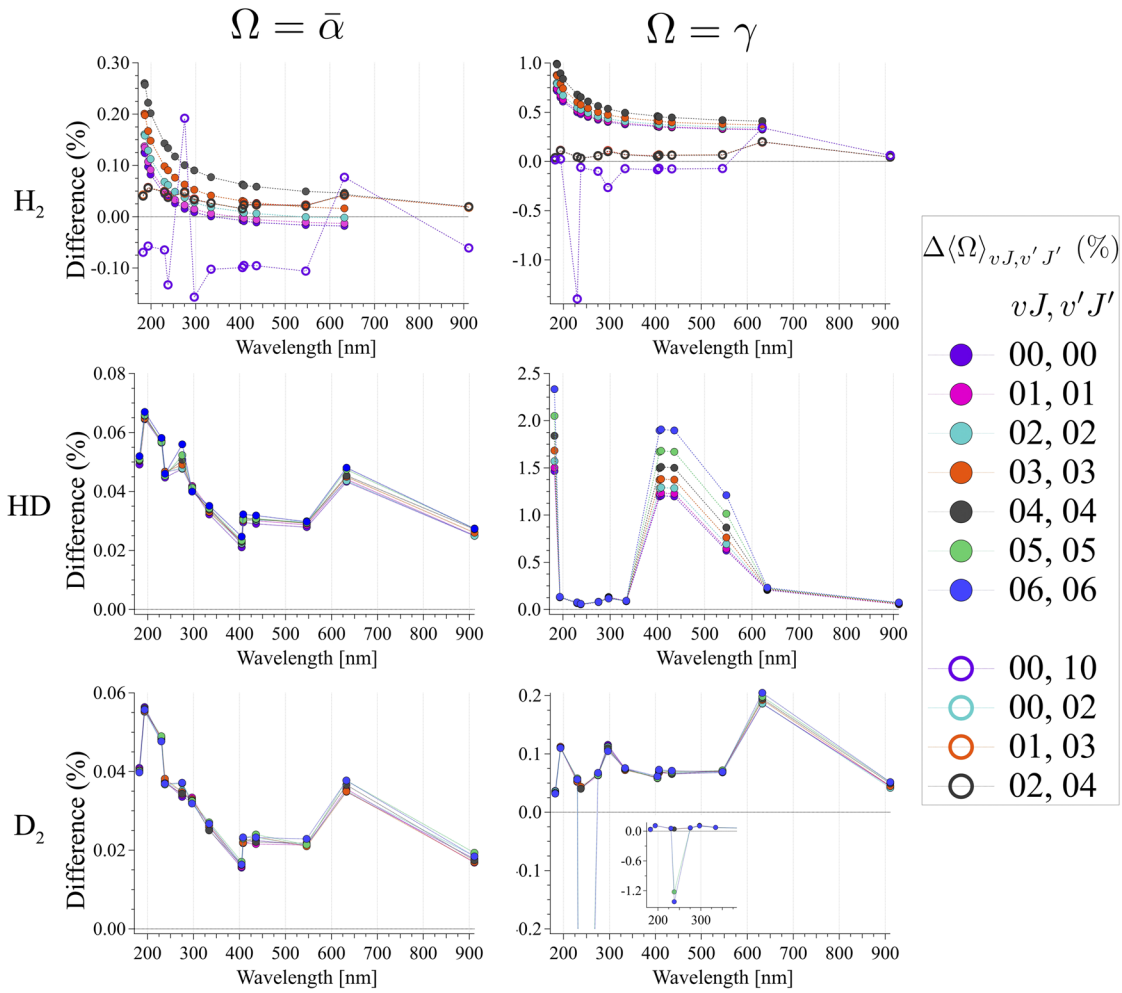

FIG. 4. Relative difference (in %) defined as $[(\langle\Omega\rangle_{vJ,v'J'} - \langle\Omega\rangle^{\mathrm{ref}}_{vJ,v'J'})/\langle\Omega\rangle^{\mathrm{ref}}_{vJ,v'J'}]$ between the present results and the reference results of Rychlewski (Ref. 27) and Bishop (Ref. 75) for the wavelength dependent matrix elements of mean polarizability ($\Omega = \bar{\alpha}$) and polarizability anisotropy ($\Omega = \gamma$). The entries for the diagonal matrix elements are marked with solid circles and for the off-diagonal matrix elements with open circles. For H_2, the reference diagonal matrix elements ($\langle 0, J|\Omega|0, J\rangle$ with $J = 0$–4) are taken from Ref. 75 and the reference off-diagonal matrix elements ($\langle 0, 0|\Omega|1, 0\rangle$ and $\langle 0, J|\Omega|0, J+2\rangle$ with $J = 0$–4) from Ref. 27. For HD and D_2, all reference entries ($\langle 0, J|\Omega|0, J\rangle$ with $J = 0$–6) are taken from Ref. 27.

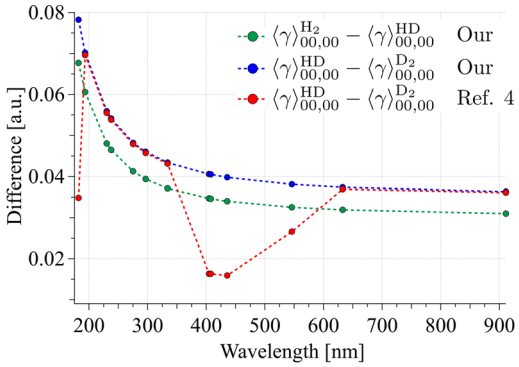

FIG. 5. Absolute differences between the wavelength dependent matrix element $\langle\gamma\rangle_{00,00}$ for H_2 and HD computed from our data (green circles) change smoothly with wavelength as anticipated for polarizability anisotropy. Similar observation concerns the analogous differences for HD and D_2 computed from our data (blue circles). However, the differences computed from the results of Rychlewski (Ref. 27, red circles) show large deviation from the expected trend at 182.26, 404.77, 407.90, 435.96, and 546.23 nm, indicating possible numerical errors in Table III of Ref. 27 for values at these wavelengths. Similar departure from the expected trend exists also for the matrix elements $\langle\gamma\rangle_{0J,0J}$ with J = 1–6 of HD.

large and irregular departures from that line, suggesting large numerical errors. The reasons for the errors in Rychlewski's work have not been identified.

- For a number of wavelengths (230.29, 275.36, and 632.80 nm) in the plots corresponding to the $\langle 0,0|\bar{\alpha}|1,0\rangle$ and $\langle 0,\ 0|\gamma|1,\ 0\rangle$ matrix elements of H_2 in Fig. 4, large numerical discrepancies have been observed between our data and the results given by Rychlewski in Ref. 27. To understand which of the two sets of data experiences numerical problems, we have plotted in Fig. 6, the ratio $\langle 0,0|\gamma|1,0\rangle/\langle 0,0|\bar{\alpha}|1,0\rangle$ as a function of laser wavelength for our data (red circles) and Rychlewski's results (blue circles). Both sets of data have been subsequently fitted to a cubic polynomial in the inverse powers of the wavelength, and the residuals of the fits (see Fig. 6) have been analyzed. The residuals of the fit corresponding to our data are of the order 10^{-5}, and the residuals corresponding to Rychlewski's results are of the order 10^{-3}, with particularly large fitting errors for the wavelengths of 230.29 and 632.80 nm. These results suggest that the discrepancies discussed here are originating from numerical noise in Rychlewski's results.
- For H_2, our results show noticeably larger systematic departure from the results of Bishop and Cheung[75] (up to 0.25% for the diagonal matrix elements over the $\bar{\alpha}$ operator and up to 1% for the diagonal matrix elements over the γ operator) than from the results of Rychlewski[27] (0.15% and 0.20%, respectively, for the off-diagonal elements after elimination of the erroneous outliers identified above). It is difficult to state unequivocally, which of these two existing sets of theoretical data is more precise as Rychlewski used larger explicitly correlated basis in his calculations, but at the same time he resorted to approximations (similarly like this work) in the averaging procedure. Close numerical resemblance of our results to the results of Rychlewski, in the light of the fact that they were obtained using drastically different approaches, suggests that the larger numerical discrepancies to the work of Bishop and Cheung[75] might be possibly ignored by treating this reference as less accurate. We discuss this issue again later, while comparing our results with the available experimental findings. We give a warning here: if more accurate polarizability matrix elements are available in the future, the discrepancy between Bishop and Cheung's and Rychlewski's results discussed here should be one of the most important issues to be re-investigated.

Another set of matrix elements $\langle v,\ J|\gamma|v,\ J+2\rangle$ with v = 0–1 and J = 0–3 and $\langle v, J|\bar{\alpha}|v+1, J\rangle$ with v = 0 and J = 0–3 was computed for H_2, HD, and D_2 at the wavelength of 488 nm by Schwartz and Le Roy.[28] Our results show close resemblance to this set of data with an almost constant difference of 0.0004 for the matrix elements involving $\bar{\alpha}$ and 0.0010 for the matrix elements involving γ. A detailed comparison is given in Table T30 of the supplementary material.

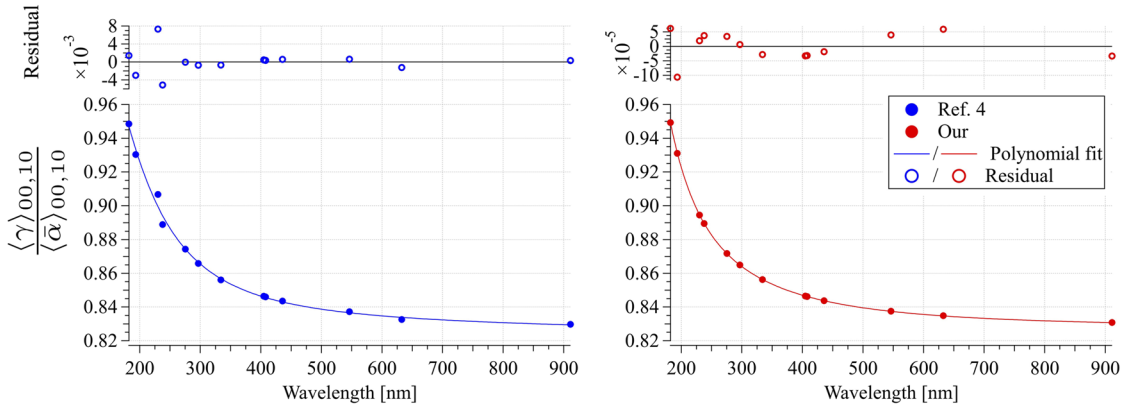

FIG. 6. Ratio $\langle\gamma_{00,10}\rangle/\langle\bar{\alpha}_{00,10}\rangle$ for H_2 plotted as a function of laser wavelength using the results by Rychlewski (Ref. 27, blue solid circles) and the present results (red solid circles). Cubic polynomial fit (blue and red lines) in inverse powers of the wavelength is used to assess the quality of both sets of data by visualizing the fitting residuals (upper panels). The fit residuals for Rychlewski's results (blue open circles) are ~100 times larger than the residuals for our results (red open circles), suggesting substantial numerical noise in respective matrix elements of H_2 in Table VII of Ref. 27.

Accurate determination of polarizability by experiment is quite a difficult task and needs special considerations when aiming at errors smaller than 2%. For this reason, the number of available experimental data is rather limited. James and co-workers[35] have measured the depolarization ratio of the Q1(J) branch given by $\rho = [3b_J^{(2)}\gamma^2/(45\bar{\alpha}^2 + 4b_J^{(2)}\gamma^2)]$, where $b_J^{(2)}$ is the Placzek-Teller factor for $\Delta J = 0$ transitions. They have reported ρ [for Q1(J) branches] for all the isotopologues of the hydrogen molecule at 532 nm while carefully correcting for polarization and geometrical aberrations. Our present results are in good agreement with their reported results tabulated in Table I.

Cureton and co-workers[10] have determined polarizability anisotropy relevant to the $v = 1$, $J = 1 \rightarrow v = 1$, $J = 3$ pure rotational Raman transition in the first vibrational state of H_2 by utilizing stimulated Raman pumping using pulsed 683 and 954 nm light for populating the $v = 1$ state and a time delayed probe laser at 355 nm for observing the spontaneous rotational Raman signal. Using the integrated band intensities of the S1(1) band to the S0(1) band ($A_{S1(1)}/A_{S0(1)}$) and employing the extrapolated experimental value of $\gamma_{01,03}$ available for 488 nm from the work of Asawaroengchai and Rosenblatt,[80] they determined the polarizability anisotropy ($\gamma_{11,13}$) at 355 nm. The value of $\gamma_{11,13}$ at 355 nm obtained by us in the current work is larger by ~17% than that reported by Cureton and co-workers (see Table II). The complexity of the scientific reasoning based on relatively simple experimental results do not allow us to state clearly what the reasons for such a large discrepancy could be. We believe that careful critical reinvestigation of the reasoning could shed some light on this issue. The theoretical value computed for the first vibrational state and reported by us in the current paper is in good agreement with the earlier analogous result reported by Schwartz and Le Roy[28] (see Table II and Table T30 of the supplementary material), suggesting that both theoretical values are likely to be correct.

MacAdam and Ramsey[78] directly measured the polarizability anisotropy of H_2 and D_2 for $J = 1$ in the ground electronic and vibrational state utilizing molecular-beam magnetic-resonance measurements. Their experimental values of $\langle\gamma\rangle_{01,01}$, 2.0353 (33) a.u. for H_2 and 1.9685 (26) a.u. for D_2, are in good agreement with the present results, 2.0390 for H_2 and 1.9695 a.u. for D_2.

Bridge and Buckingham[79] reported the Rayleigh depolarization ratio ($\kappa = \gamma/3\bar{\alpha}$) of laser beam scattered by different gases including H_2 and D_2. In their work, the Rayleigh depolarization ratio has been carefully determined at 632.8 nm using a specially designed cell placed inside a laser cavity while taking care to remove the effect from dust particles, reflections from the gas-cell windows, as well as the small contributions from Raman scattering in the case of H_2. This allowed for very accurate experimental determination of the depolarization ratio from which the polarizability in the ground state was derived. The depolarization ratio was found to be 0.128 ± 0.002 for H_2 and 0.123 ± 0.002 for D_2. Our present values of these ratios, 0.1264 for H_2 and 0.1238 for D_2, are within the experimental errors. A detailed comparison of our mean polarizability and anisotropy matrix elements computed at 632.8 nm with the analogous experimental results of Bridge and Buckingham reported in Ref. 79 is given in Table II.

Asawaroengchai and Rosenblatt[80] determined the value of the first derivative of the polarizability anisotropy $\langle\gamma_1/\gamma_0\rangle_{r_e}$ for H_2 and D_2 at the equilibrium internuclear distance using 488 nm laser and a tungsten lamp for intensity calibration. Hamaguchi and co-workers[81,86] determined the first and the second derivatives of the polarizability anisotropy ($\langle\gamma_1/\gamma_0\rangle_{r_e}$ and $\langle\gamma_2/\gamma_{0_{r_e}}\rangle$) for H_2 and D_2 using laser wavelengths from 476.5 to 514.5 nm. These results were obtained using a non-linear least squares regression analysis of the observed experimental intensities and, in addition to the set of the derivatives, simultaneously yielded the response function of the spectrometer in the considered spectral window. We have extracted similar derivatives for H_2 and D_2 and their expectation values from the results obtained in the current study. We have computed analogous first and second derivatives for H_2 at 476.5, 488, and 496.5 nm and for D_2 at 514.5 nm using our results and have averaged them to compare with the results of Hamaguchi *et al.* The comparison for the first and the second derivatives, shown in Table II, shows satisfactory agreement between the experimental and theoretical results.

Victor and Dalgarno[82] listed the derived thermally averaged dynamic mean polarizabilites in the ground vibrational state at several wavelengths spanning 185.46–632.8 nm using data from the existing literature on refractive indices[84,85] and polarizability.[83] These thermally averaged dynamic mean polarizabilites are compared with our computed results (after thermal averaging) in Table II where the present values are larger up to 0.3%, indicating good correspondence between both sets of data.

Theoretical results by Bishop and Cheung[75] for thermally averaged mean polarizability and anisotropy are shown in Table II, where the disagreement with our results shows

TABLE I. Comparison of the theoretical and experimental depolarization ratios of the Q1 branch of H_2, HD, and D_2 at 532 nm.

	H_2			HD			D_2		
	Theory		Expt.	Theory		Expt.	Theory		Expt.
J	Our	Reference 35	Reference 35	Our	Reference 35	Reference 35	Our	Reference 35	Reference 35
1	0.0183	0.0183	0.0177(6)	0.0177	0.0176	0.0174(6)	0.0180	0.0180	0.0177(6)
2	0.0133	0.0132	0.0133(6)	0.0127	0.0127	0.0118(6)	0.0130	0.0130	0.0126(6)
3	0.0125	0.0125	0.0128(6)	0.0120	0.0119	0.0112(6)	0.0122	0.0122	0.0121(6)

TABLE II. Comparison of available theoretical and experimental results for the mean polarizability and anisotropy.

Molecule	Property	λ (nm)	Theory		Expt.
			Our	Reference 10[a]	Reference 10
H_2	$\langle\gamma\rangle_{01,03}$	355	2.2771	2.2819	
	$\langle\gamma\rangle_{11,13}$		2.8413	2.8228	2.411(28)
			Our		Reference 78
H_2	$\langle\gamma\rangle_{01,01}$	Static	2.0390		2.0353(33)
D_2	$\langle\gamma\rangle_{01,01}$	Static	1.9695		1.9685(26)
			Our		Reference 79
H_2	$\langle\bar{\alpha}\rangle_{00,00}$	632.8	5.5232		5.527(27)
	$\langle\gamma\rangle_{00,00}$		2.0947		2.119(10)
D_2	$\langle\bar{\alpha}\rangle_{00,00}$	632.8	2.0254		2.018(10)
	$\langle\gamma\rangle_{00,00}$		5.4514		5.459(27)
			Our		Reference 80
H_2	$\langle\gamma_1/\gamma_0\rangle_{00,00}$	488	2.6769		2.63(0.07)
D_2	$\langle\gamma_1/\gamma_0\rangle_{00,00}$	488	2.6778		2.63(0.07)
			Our		Reference 81[b]
H_2	$\langle\gamma_1/\gamma_0\rangle_{00,00}$	476.6, 488, 496.5	2.6772		2.53(0.13)
	$\langle\gamma_2/\gamma_0\rangle_{00,00}$	476.6, 488, 496.5	4.8997		3.97(1.33)
D_2	$\langle\gamma_1/\gamma_0\rangle_{00,00}$	514.5	2.6713		2.53(0.13)
	$\langle\gamma_2/\gamma_0\rangle_{00,00}$	514.5	4.8763		3.97(1.33)
			Our[c]	Reference 75[d]	Reference 82[e]
H_2	$\langle\bar{\alpha}\rangle$ av[f]	185.46	7.0548	7.0445	7.035
		186.27	7.0358	7.0257	7.017
		193.58	6.8792	6.8712	6.868
		199.05	6.7777	6.7709	6.771
		230.29	6.3693	6.3655	6.384
		237.91	6.2993	6.2961	6.303
		253.56	6.1792	6.1767	6.183
		275.36	6.0509	6.0491	6.055
		296.81	5.9553	5.9540	5.960
		334.24	5.8355	5.8348	5.840
		404.77	5.7003	5.7002	5.705
		407.90	5.6960	5.6959	5.701
		435.96	5.6617	5.6617	5.667
		546.23	5.5762	5.5765	5.582
		632.80	5.5389	5.5394	5.554
			Our[c]	Reference 75[d]	
H_2	$\langle\gamma\rangle$av[f]	185.46	3.1183	3.0946	
		186.27	3.1045	3.0811	
		193.58	2.9922	2.9717	
		199.05	2.9203	2.9016	
		230.29	2.6397	2.6258	
		237.91	2.5929	2.5797	
		253.56	2.5134	2.5014	
		275.36	2.4296	2.4188	
		296.81	2.3680	2.3580	
		334.24	2.2918	2.2827	
		404.77	2.2071	2.1990	
		407.90	2.2044	2.1963	
		435.96	2.1831	2.1753	
		546.23	2.1305	2.1232	
		632.80	2.1077	2.1006	

[a]Extrapolated results derived from data given in Ref. 28.
[b]H_2 measured using the 476.5, 488, and 496.5 nm laser. D_2 measured using the 514.5 nm laser. All the Raman intensity data from H_2 and D_2 were treated together to extract the derivatives.
[c]Averaging up to $v = 0$, $J = 7$ at 293 K.
[d]Averaging up to $v = 0$, $J = 4$ at 293 K.
[e]Derived from results given in Refs. 83–85.
[f]Thermal rotational average.

wavelength dependent change, as also visualized in Fig. 4 (for diagonal matrix elements of $\bar{\alpha}$ and γ) for H_2. Even so, the maximum difference is less than 0.2% for thermally averaged mean polarizability and less than 0.8% for thermally averaged anisotropy. It is difficult to ascertain which of the two (present or the work of Bishop and Cheung) is more reliable while estimating the plausible source(s) of errors.

In general, the agreement between our calculations and the available theoretical (Fig. 4 and Table T30 in the supplementary material) and experimental (Tables I and II) results is rather good, except for the results reported in Ref. 10 by Cureton and co-workers.

A detailed analysis of various sources of errors in the computational procedure employed in the current study is presented in Sec. S6 of the supplementary material. The computed matrix elements are accurate to about 10^{-3}, and for that reason we tabulate them in Tables T1–T15 of the supplementary material only up to four digits after the decimal point. The major error component in the presented matrix elements originates from the inaccuracies in the polarizability invariants. Note that the current accuracy is sufficient for our main goal of developing a universal standard for determining absolute Raman cross sections and absolute Raman intensities needed for quantitative Raman spectroscopy, where currently the routine measurements have a typical error of the order of ~4%-5%. Our goal is to reduce this uncertainty to ~1%-2%, which should be possible with our theoretical data.

V. CONCLUSIONS

We present an exhaustive compilation of frequency dependent polarizability rovibrational matrix elements relevant in the context of Rayleigh and Raman scattering experiments for H_2, HD, and D_2. The matrix elements, accurate to about 10^{-3}, can be computed by a numerical integration routine provided by us for any excitation wavelengths in the interval 182.25–1320.6 nm and for any rovibrational states with $J = 0$–15 and $v = 0$–4. An extensive compilation of various matrix elements evaluated in this way for 52 various excitation wavelengths between 182.25 and 1320.6 nm corresponding to the frequencies of commercially available lasers is given in Tables T1–T15 of the supplementary material. The dynamic polarizabilities are determined from CCSD calculations using an augmented sextuple-zeta basis set with additional custom bond-functions designed to achieve high accuracy. The set of rovibrational wave functions for the electronic ground state of H_2, HD, and D_2 is determined by solving numerically the radial-nuclear equation, using the clamped nuclei potential energy surface with adiabatic, relativistic, and radiative corrections computed by Wolniewicz.[38] The tabulated matrix elements extend substantially the data available in the literature, both with respect to the number of rovibrational states covered and the number of reported laser frequencies, allowing us also to identify and correct a number of numerical or procedural errors in the previously published results.

The reported matrix elements can be used to straightforwardly calculate the Rayleigh and Raman cross sections,[2–4,103,104] leading to the intensities of Rayleigh and Raman bands which allows for the accurate quantitative Raman spectroscopy of molecular hydrogen applicable to the studies of flames[18,20] and catalysis.[87,88] Calculation of the accurate band intensity also gives the depolarization ratios.[35,89] Moreover, several important wavelength dependent physical properties such as refractive indices,[82,84,85] Verdet[90,91] and Kerr constants[92–94] can be readily computed using the matrix elements.

From our perspective, the possibility of theoretical determination of accurate Raman band intensities provides an excellent opportunity for assessing the performance of Raman spectrometers and for their careful and accurate calibration.[6,7] The knowledge of the depolarization ratios of these molecules allows for the simultaneous correction for the polarization dependence of spectrometer's sensitivity. A calibrated Raman spectrometer can be used for many kinds of precise experiments, for example, absolutely quantitative Raman spectroscopy provided the Raman cross section for the specific marker band of the molecule of study is known,[5] experimental determination of Raman and Rayleigh cross sections,[3,11–13,95,96] determination of temperature at the sampling point using the measured anti-Stokes and Stokes Raman intensities,[5,14–23] analysis of the population distribution among rovibrational states necessary to understand relaxation and energy transfer processes[8] and population transfer among rovibrational states[9,10,97] studied using Raman spectroscopy.

In general, the calculated Raman band intensities can be used to calibrate spectrometers involving photon detection, provided the wavelength ranges are appropriate to measure a few Raman bands from hydrogen isotopologues (or other molecules whose Raman cross sections are known) using a laser of suitable wavelength, for example, the calibration of the fluorescence spectrometer using H_2[98,99] and Thomson scattering spectrometers[33,34,36] calibrated using pure rotational Raman bands of H_2 and D_2. Thus, the present set of wavelength dependent matrix elements enables such applications for calibration procedures involving H_2, HD, and D_2.

The thorough compilation of matrix elements reported in this study thus has wide applications, and the present work constitutes the first step in the process of developing a universal standard for Raman intensities based on the rovibrational transitions in H_2, HD, and D_2.

SUPPLEMENTARY MATERIAL

See supplementary material for the following additional content: (S1) matrix elements of mean polarizability, $\bar{\alpha} = (2\alpha_\perp + \alpha_\parallel +)/3$; (S2) matrix elements of polarizability anisotropy, $\gamma = (\alpha_\parallel - \alpha_\perp)$; (S3) static polarizability components and invariants for H_2 at selected distances; (S4) development of the bond functions used in this work; (S5) details of the numerical procedure used for the solution of the 1D Schrödinger equation (along with a comparison with the results obtained by the Cooley method[100,101]); (S6) error estimation for matrix elements; (S7) tables of the computed dissociation and transitions energies of H_2, D_2, and HD; and (S8) comparison of rotationally averaged mean polarizability and anisotropy with previous results.

ACKNOWLEDGMENTS

Ministry of Science and Technology (Grant Nos. MOST105-2113-M-009-018-MY3 and MOST103-2113-M-009-001) and Ministry of Education (MOE-ATU project) of Taiwan are acknowledged for financial support.

APPENDIX: SOFTWARE AND DATA AVAILABILITY

Programs for computation of rovibrational matrix elements along with the polarizability data ($\alpha_\perp$ and $\alpha_\parallel$) and rovibrational wave functions are available on GitHub[39] and as the supplementary material with a detailed tutorial on usage. Computation of static and wavelength dependent matrix elements matrix elements of polarizability perpendicular to the internuclear axis ($\alpha_\perp$), polarizability parallel to the internuclear axis ($\alpha_\parallel$), mean polarizability ($\bar{\alpha} = (2\alpha_\perp + 2\alpha_\parallel)/3$), and the anisotropy ($\gamma = \alpha_\parallel - \alpha_\perp$) for H_2, HD, and D_2 in $v = 0$–4 and $J = 0$–15 can be performed using these tools.

[1] G. Placzek, *Handbuch der Radiologie* (Akademische Verlagsgesellschaft, 1934), Vol. 2, p. 209.
[2] A. L. Ford and J. C. Browne, At. Data Nucl. Data Tables **5**, 305 (1973).
[3] R. W. Carlson and W. R. Fenner, Astrophys. J. **178**, 551 (1972).
[4] Y. Udagawa, N. Mikami, K. Kaya, and M. Ito, J. Raman Spectrosc. **1**, 341 (1973).
[5] J. M. Fernández, A. Punge, G. Tejeda, and S. Montero, J. Raman Spectrosc. **37**, 175 (2006).
[6] H. Hamaguchi, I. Harada, and T. Shimanouchi, Chem. Lett. **3**, 1405 (1974).
[7] M. Schlösser, S. Rupp, H. Seitz, S. Fischer, B. Bornschein, T. M. James, and H. H. Telle, J. Mol. Struct. **1044**, 61 (2013).
[8] J. Arnold, T. Dreier, and D. W. Chandler, Chem. Phys. **133**, 123 (1989).
[9] D. J. Saiki, S. Cureton-Chinn, P. B. Kelly, and M. P. Augustine, J. Chem. Phys. **123**, 104311 (2005).
[10] S. M. Cureton, S. Vyas, P. B. Kelly, and M. P. Augustine, Mol. Phys. **98**, 349 (2000).
[11] Y. Kato and H. Takuma, J. Opt. Soc. Am. **61**, 347 (1971).
[12] H. A. Hyatt, J. M. Cherlow, W. R. Fenner, and S. P. S. Porto, J. Opt. Soc. Am. **63**, 1604 (1973).
[13] C. M. Penney, R. L.S. Peters, and M. Lapp, J. Opt. Soc. Am. **64**, 712 (1974).
[14] J. J. Barrett and A. Weber, J. Opt. Soc. Am. **60**, 70 (1970).
[15] J. A. Salzman, W. J. Masica, and T. A. Coney, Technical Report NASA TN D-6336, 1971.
[16] R. S. Hickman and L. H. Liang, Rev. Sci. Instrum. **43**, 796 (1972).
[17] M. C. Drake and G. M. Rosenblatt, Chem. Phys. Lett. **44**, 313 (1976).
[18] M. C. Drake and J. W. Hastie, Combust. Flame **40**, 201 (1981).
[19] W. Kreutner, W. Stricker, and T. Just, Ber. Bunsengesellschaft Phys. Chem. **87**, 1045 (1983).
[20] W. Reckers, L. Hüwel, G. Grünefeld, and P. Andresen, Appl. Opt. **32**, 907 (1993).
[21] G. Zikratov, F.-Y. Yueh, J. P. Singh, O. P. Norton, R. A. Kumar, and R. L. Cook, Appl. Opt. **38**, 1467 (1999).
[22] J. Kojima and Q. V. Nguyen, Meas. Sci. Technol. **15**, 565 (2004).
[23] A. V. Sepman, V. V. Toro, A. V. Mokhov, and H. B. Levinsky, Appl. Phys. B **112**, 35 (2013).
[24] Several symbols have been used to represent mean polarizability [$(\alpha_\parallel + 2\alpha_\perp)/3$] and polarizability anisotropy ($\alpha_\perp - \alpha_\parallel$) in the existing literature. In the present work, we choose to represent the mean polarizability by $\bar{\alpha}$ and the polarizability anisotropy by γ, following the standard Refs. 3, 10, 23, 25–27, 45, 81, 86, and 102 and textbooks.[103,104] Note that other choices are also popular in the literature, including α for the mean polarizability and β for the polarizability anisotropy.[80,105,106]
[25] W. Kołos and L. Wolniewicz, J. Chem. Phys. **46**, 1426 (1967).
[26] A. L. Ford and J. C. Browne, Phys. Rev. A **7**, 418 (1973).
[27] J. Rychlewski, J. Chem. Phys. **78**, 7252 (1983).
[28] C. Schwartz and R. J. Le Roy, J. Mol. Spectrosc. **121**, 420 (1987).
[29] W. Kołos, K. Szalewicz, and H. J. Monkhorst, J. Chem. Phys. **84**, 3278 (1986).
[30] W. Kołos and L. Wolniewicz, J. Chem. Phys. **41**, 3663 (1964).
[31] D. M. Bishop and L. M. Cheung, J. Chem. Phys. **69**, 1881 (1978).
[32] L. Wolniewicz, J. Chem. Phys. **78**, 6173 (1983).
[33] T. Yamauchi and I. Yanagisawa, Appl. Opt. **24**, 700 (1985).
[34] F. Flora and L. Giudicotti, Appl. Opt. **26**, 4001 (1987).
[35] T. M. James, M. Schlösser, S. Fischer, M. Sturm, B. Bornschein, R. J. Lewis, and H. H. Telle, J. Raman Spectrosc. **44**, 857 (2013).
[36] H. Röhr, Phys. Lett. A **81**, 451 (1981).
[37] D. M. Bishop, Rev. Mod. Phys. **62**, 343 (1990).
[38] L. Wolniewicz, J. Chem. Phys. **99**, 1851 (1993).
[39] See https://github.com/ankit7540/H2-PolarizabilityMatrixElements for the repository containing a FORTRAN program, a python module along with polarizability data and rovibrational wave functions, for the calculation of rovibrational matrix elements of polarizability for H_2, HD, and D_2; accessed 18-01-2017.
[40] O. Christiansen, A. Halkier, H. Koch, P. Jørgensen, and T. Helgaker, J. Chem. Phys. **108**, 2801 (1998).
[41] K. Aidas, C. Angeli, K. L. Bak, V. Bakken, R. Bast, L. Boman, O. Christiansen, R. Cimiraglia, S. Coriani, P. Dahle, E. K. Dalskov, U. Ekström, T. Enevoldsen, J. J. Eriksen, P. Ettenhuber, B. Fernández, L. Ferrighi, H. Fliegl, L. Frediani, K. Hald, A. Halkier, C. Hättig, H. Heiberg, T. Helgaker, A. C. Hennum, H. Hettema, E. Hjertenæs, S. Høst, I. M. Høyvik, M. F. Iozzi, B. Jansík, H. J. A. Jensen, D. Jonsson, P. Jørgensen, J. Kauczor, S. Kirpekar, T. Kjærgaard, W. Klopper, S. Knecht, R. Kobayashi, H. Koch, J. Kongsted, A. Krapp, K. Kristensen, A. Ligabue, O. B. Lutnæs, J. I. Melo, K. V. Mikkelsen, R. H. Myhre, C. Neiss, C. B. Nielsen, P. Norman, J. Olsen, J. M. H. Olsen, A. Osted, M. J. Packer, F. Pawlowski, T. B. Pedersen, P. F. Provasi, S. Reine, Z. Rinkevicius, T. A. Ruden, K. Ruud, V. V. Rybkin, P. Sałek, C. C. M. Samson, A. S. de Merás, T. Saue, S. P. A. Sauer, B. Schimmelpfennig, K. Sneskov, A. H. Steindal, K. O. Sylvester-Hvid, P. R. Taylor, A. M. Teale, E. I. Tellgren, D. P. Tew, A. J. Thorvaldsen, L. Thøgersen, O. Vahtras, M. A. Watson, D. J. D. Wilson, M. Ziolkowski, and H. Ågren, Wiley Interdiscip. Rev.: Comput. Mol. Sci. **4**, 269 (2014).
[42] S. L. Mielke, B. C. Garrett, and K. A. Peterson, J. Chem. Phys. **116**, 4142 (2002).
[43] D. Feller, J. Comput. Chem. **17**, 1571 (1996).
[44] K. L. Schuchardt, B. T. Didier, T. Elsethagen, L. Sun, V. Gurumoorthi, J. Chase, J. Li, and T. L. Windus, J. Chem. Inf. Model. **47**, 1045 (2007).
[45] J. Rychlewski, Mol. Phys. **41**, 833 (1980).
[46] F. Tao and Y. Pan, J. Chem. Phys. **97**, 4989 (1992).
[47] F. Tao, J. Chem. Phys. **100**, 3645 (1994).
[48] F. Tao, J. Chem. Phys. **100**, 4947 (1994).
[49] F. Tao and W. Klemperer, J. Chem. Phys. **103**, 950 (1995).
[50] H. L. Williams, E. M. Mas, K. Szalewicz, and B. Jeziorski, J. Chem. Phys. **103**, 7374 (1995).
[51] J. S. Wright and E. Kruus, J. Chem. Phys. **85**, 7251 (1986).
[52] J. S. Wright and V. J. Barclay, J. Chem. Phys. **86**, 3054 (1987).
[53] J. S. Wright and V. J. Barclay, J. Comput. Chem. **12**, 697 (1991).
[54] R. D. Bardo and K. Ruedenberg, J. Chem. Phys. **60**, 918 (1974).
[55] S. Huzinaga, M. Klobukowski, and H. Tatewaki, Can. J. Chem. **63**, 1812 (1985).
[56] P. J. Mohr, D. B. Newell, and B. N. Taylor, "The 2014 CODATA recommended values of the fundamental physical constants" web version 7.2 (National Institute of Standards and Technology, Gaithersburg, MD, 2016), available: http://physics.nist.gov/constants; accessed 31-10-2017 00:05:18 EDT.
[57] J. Komasa, K. Piszczatowski, G. Łach, M. Przybytek, B. Jeziorski, and K. Pachucki, J. Chem. Theory Comput. **7**, 3105 (2011).
[58] K. Pachucki and J. Komasa, Phys. Chem. Chem. Phys. **12**, 9188 (2010).
[59] J. Liu, D. Sprecher, C. Jungen, W. Ubachs, and F. Merkt, J. Chem. Phys. **132**, 154301 (2010).
[60] Y. P. Zhang, C. H. Cheng, J. T. Kim, J. Stanojevic, and E. E. Eyler, Phys. Rev. Lett. **92**, 203003 (2004).
[61] D. Jennings and J. Brault, J. Mol. Spectrosc. **102**, 265 (1983).
[62] D. E. Jennings, A. Weber, and J. W. Brault, Appl. Opt. **25**, 284 (1986).
[63] N. H. Rich, J. W. C. Johns, and A. R. W. McKellar, J. Mol. Spectrosc. **95**, 432 (1982).
[64] S. Bragg, J. Brault, and W. Smith, Astrophys. J. **263**, 999 (1982).
[65] M. Stanke, S. Bubin, M. Molski, and L. Adamowicz, Phys. Rev. A **79**, 032507 (2009).
[66] A. R. W. McKellar and T. Oka, Can. J. Phys. **56**, 1315 (1978).
[67] L. Wolniewicz, J. Chem. Phys. **103**, 1792 (1995).
[68] D. K. Veirs and G. M. Rosenblatt, J. Mol. Spectrosc. **121**, 401 (1987).
[69] Igor Pro, WaveMetrics, Lake Oswego, OR, USA, A scientific data analysis software with numerical computing environment and a programming language.

[70]T. N. L. Patterson, Math. Comput. **22**, 847 (1968).
[71]T. N. L. Patterson, Math. Comput. **23**, 892 (1969).
[72]R. Piessens, E. de Doncker-Kapenga, C. Überhuber, and D. Kahaner, *Quadpack—A Subroutine Package for Automatic Integration* (Springer-Verlag Berlin Heidelberg, 1983).
[73]W. H. Press, S. A. Teukolsky, B. P. Flannery, and W. T. Vetterling, *Numerical Recipes in Fortran (The Art of Scientific Computing)* (Cambridge University Press, 1993), Vol. 2, pp. 140–150.
[74]T. Renner, in *Quantities, Units and Symbols in Physical Chemistry*, edited by E. R. Cohen, T. Cvitas, J. G. Frey, B. Holstrom, K. Kuchitsu, R. Marquardt, I. Mills, F. Pavese, M. Quack, J. Stohner, H. L. Strauss, M. Takami, and A. J. Thor (Royal Society of Chemistry, 2007), pp. 1–232.
[75]D. M. Bishop and L. M. Cheung, J. Chem. Phys. **72**, 5125 (1980).
[76]J. Rychlewski, Chem. Phys. Lett. **73**, 135 (1980).
[77]Unpublished results by Ankit Raj, where the $v = 0, J = 6 \rightarrow v = 0, J = 8$ (H_2); $v = 0, J = 6 \rightarrow v = 0, J = 8$ (HD); and $v = 0, J = 8 \rightarrow v = 0, J = 10$ (D_2) transitions have been observed.
[78]K. B. MacAdam and N. F. Ramsey, Phys. Rev. A **6**, 898 (1972).
[79]N. J. Bridge and A. D. Buckingham, Proc. R. Soc. A **295**, 334 (1966).
[80]C. Asawaroengchai and G. M. Rosenblatt, J. Chem. Phys. **72**, 2664 (1980).
[81]H.-O. Hamaguchi, A. Buckingham, and W. Jones, Mol. Phys. **43**, 1311 (1981).
[82]G. A. Victor and A. Dalgarno, J. Chem. Phys. **50**, 2535 (1969).
[83]N. J. Bridge and A. D. Buckingham, J. Chem. Phys. **40**, 2733 (1964).
[84]J. Koch, Ark. Math. Astron. Fys. **8**, 20 (1912).
[85]M. Kirn, Ann. Phys. **64**, 566 (1921).
[86]H.-O. Hamaguchi, I. Suzuki, and A. Buckingham, Mol. Phys. **43**, 963 (1981).
[87]S. E. Jones, D. S. Shelton, R. S. Turley, M. J. Lawler, and D. D. Allred, Hyperfine Interact. **101**, 695 (1996).
[88]Y. G. Lü, Z. J. Li, L. Z. Wu, P. Wang, L. M. Fu, and J. P. Zhang, Acta Phys. Chim. Sin. **29**, 1632 (2013).
[89]D. M. Golden and B. Crawford, Jr., J. Chem. Phys. **36**, 1654 (1962).
[90]H. Becquerel, C. R. Acad. Sci. **125**, 679 (1897).
[91]W. A. Parkinson, S. P. A. Sauer, and J. Oddershede, J. Chem. Phys. **98**, 487 (1993).
[92]R. Tammer and W. Hüttner, Chem. Phys. **146**, 155 (1990).
[93]R. Tammer, K. Löblein, K. H. Peting, and W. Hüttner, Chem. Phys. **168**, 151 (1992).
[94]S. C. Read, A. D. May, and G. D. Sheldon, Can. J. Phys. **75**, 211 (1997).
[95]K. T. Schomacker, J. K. Delaney, and P. M. Champion, J. Chem. Phys. **85**, 4240 (1986).
[96]G. W. Faris and R. A. Copeland, Appl. Opt. **36**, 2686 (1997).
[97]S. Cureton-Chinn, P. B. Kelly, and M. P. Augustine, J. Chem. Phys. **116**, 4837 (2002).
[98]W. K. Bischel, D. J. Bamford, and L. E. Jusinski, Appl. Opt. **25**, 1215 (1986).
[99]V. Sivaprakasam and D. K. Killinger, J. Opt. Soc. Am. B **20**, 1980 (2003).
[100]J. W. Cooley, Math. Comput. **15**, 363 (1963).
[101]R. J. Le Roy, J. Quant. Spectrosc. Radiat. Transfer **186**, 167 (2017).
[102]J. Rychlewski, J. Chem. Phys. **81**, 6007 (1984).
[103]D. A. Long, *The Raman Effect: A Unified Treatment of the Theory of Raman Scattering by Molecules* (John Wiley Sons Ltd., Chichester, England, 2002).
[104]E. Smith and G. Dent, *Modern Raman Spectroscopy—A Practical Approach* (John Wiley Sons Ltd., Chichester, England, 2005).
[105]W. F. Murphy, J. Raman Spectrosc. **11**, 339 (1981).
[106]T. C. James and W. Klemperer, J. Chem. Phys. **31**, 2664 (1959).